

Much of the recent effort of the NILM research community has been focused on improving the efficiency of prediction algorithms and computational speed, usually by presenting novel model architectures [24, 22] or even trying unconventional approaches such as finite state machines [25] and hybrid programming [26].

However, fewer works are devoted to investigating the formulation of the problem, and how this can affect the algorithm’s performance. For instance, uniformization of evaluation metrics for easy comparison of different models has been stressed in [27, 28], while the dependence on sampling frequency has been treated in [29]. This becomes a relevant issue when trying to leverage theoretical NILM results on high frequency benchmark datasets to real life scenarios where records are sampled at lower rates.

NILM datasets typically include both the aggregated power load and that of each monitored device, but not the device status (i.e. whether it is ON or OFF). Thus, a regression problem to predict the consumption of each device is naturally defined by the data. However, most works in NILM address the classification problem of determining whether the device is ON or OFF, rather than its consumption at each time interval. Defining a classification problem requires establishing a threshold or some procedure to determine the output categorical variable from the continuous output power load. Our main observation is that this process involves an external choice of thresholding method which is not included in the initial problem formulation. Depending on how this preprocessing step is performed, the performance and interpretation of the final results may vary in a significant manner. The main contribution of this paper is to highlight this matter and to discuss several possible ways to define a classification problem from the native regression problem.

The paper is organized as follows: in Section 2 we formally introduce the necessary notation to define regression and classification problems for time series in supervised learning. Section 3 introduces three different thresholding methods. Two different deep learning models are introduced and explained in Section 4. The purpose of studying two different models is to have more robust results and to ensure that the reported variations are not model dependent. The detailed methodology is carefully explained in Section 5, including data preprocessing, definition of training, validation and test sets, loss functions, optimization algorithms, and evaluation metrics. The results are exhibited in Section 6 for three monitored devices with different characteristics. Together with the results, we include a discussion on the criteria to choose the most convenient thresholding method. In section 7 we introduce architectures that optimize both classification and regression, to see how the two formulations interplay. Finally, we gather concluding remarks and outline open research problems in Section 8.

2 Problem Formulation

NILM is formulated as a supervised learning problem, where the model is trained to take the aggregate power as input signal and predict the power or state (ON/OFF) of each monitored appliance. This power load is measured by the smart meter at a constant rate τ^* , which produces a series of power measurements³ P_i at each sampled interval. For the analysis, it is often convenient to resample the original series at a larger sampling interval τ , which is part of the preprocessing step. For instance, in this paper the native sampling interval for the UK-DALE dataset provided by the meters is $\tau^* = 6s$, but we choose to resample the series at intervals of $\tau = 60s$.

The aggregate power P_j at instant j is the sum over all appliances:

$$P_j = \sum_{\ell=1}^L P_j^{(\ell)} + e_j, \quad (1)$$

where L is the total number of appliances in the building, $P_j^{(\ell)}$ is the power of appliance ℓ at time j , and e_j is the unidentified residual load. All of these quantities are expressed in watts.

After resampling, the training set comprises a sequence of n_{tot} records that we label as $\{P_i\}_{i=0}^{n_{tot}}$. This series is split in chunks of size n that we group in vectors as $\mathbf{P}_j = (P_{jn}, P_{j(n+1)}, \dots, P_{j(n+n-1)})$. We have a total of $n_{train} = n_{tot}/n$ such series, each of which will be an input to the model. The output of the model are sequences $\mathbf{P}_j^{(\ell)}$ for each monitored appliance over the same time intervals. The pairs $\{\mathbf{P}_j, \mathbf{P}_j^{(\ell)}\}_{j=1}^{n_{train}}$ are considered as independent points in the training set.

Supervised learning problems are usually referred to as classification or regression problems depending on whether the output variables are categorical or continuous. In the NILM literature, both of these approaches have been considered in different contributions, but there has been hardly no works devoted to the interplay between both formulations. It is precisely this gap that we would like to fill with this analysis.

³Strictly speaking, smart meters measure the energy consumption during the interval $(t, t + \tau^*)$ divided by the length of the interval τ^* .

In the *regression approach*, the predicted quantities are the power load $\mathbf{P}_j^{(\ell)}$ for each device.

In the *classification approach* the focus is on predicting whether a given appliance is at time j in a number of possible states, typically ON or OFF. We assume therefore, for the sake of simplicity, that the appliance ℓ can be in one of two states at time j , which are $s_j^{(\ell)} = 0$ (OFF state) and $s_j^{(\ell)} = 1$ (ON state). It is not evident to ascertain when a given appliance is ON or OFF by just looking at the power load. Thus, the usual criterion is to establish a threshold $\lambda^{(\ell)}$ for each appliance, and define

$$s_j^{(\ell)} = I(P_j^{(\ell)} \geq \lambda^{(\ell)}). \quad (2)$$

Multi-state classification problems, where appliances may have more than one ON status (each of them with a different consumption) have also been considered in the literature [30]. A correct definition of the classification approach thus involves a choice of threshold $\lambda^{(\ell)}$ for each appliance ℓ . Ideally, this threshold should be determined by the series of data $\mathbf{P}_j^{(\ell)}$ alone, rather than being externally fixed by human intervention. In this paper we review different algorithms to determine this threshold, which lead to rather different outcomes depending on the complexity of the input signal. We address these methods in the following section.

3 Thresholding

In this section we will explore different methods on how to set a threshold to determine the OFF and ON status of an appliance, given its input power signal.

3.1 Middle-Point Thresholding (MP)

In Middle-Point thresholding we consider the set of all power values from appliance ℓ in the training set $\{P_j^{(\ell)}\}_{j=1}^{n_{tot}}$. We apply a clustering algorithm to split this set into two clusters and consider the centroid of each cluster. Typically, the k -means clustering algorithm can be applied for this purpose, [31]. The two centroids for each class, after applying k -means, are denoted by $m_0^{(\ell)}$ (for the OFF state) and $m_1^{(\ell)}$ (for the ON state). In Middle-Point thresholding (MP), the threshold for appliance ℓ is fixed at the middle point between these values

$$\lambda^{(\ell)} = \frac{m_0^{(\ell)} + m_1^{(\ell)}}{2}. \quad (3)$$

3.2 Variance-Sensitive Thresholding (VS)

Variance-Sensitive (VS) thresholding was recently proposed as a finer version of MP thresholding by Desai et al.,[30]. It also employs k -means clustering to find the centroids for each class, but the determination of the threshold now takes into account not only the mean, but also the standard deviation $\sigma_k^{(\ell)}$ for the points in each cluster, according to the following formula

$$d = \frac{\sigma_0^{(\ell)}}{\sigma_0^{(\ell)} + \sigma_1^{(\ell)}} \quad (4)$$

$$\lambda^{(\ell)} = (1 - d)m_0^{(\ell)} + dm_1^{(\ell)}$$

The motivation is that, if $\sigma_1 > \sigma_0$, then the threshold should move towards m_0 in order not to misclassify the points in class 1 that are further away from the centroid m_1 . As a matter of fact, points in the OFF cluster usually have less variance, so the VS approach often sets its threshold lower than the MP approach. A comparison of both thresholding methods on a specific set of power measurements can be seen in Figure 1. Also note that MP is a particular case of VS when $\sigma_0 = \sigma_1$.

3.3 Activation-Time Thresholding

The last two methods only use data from the distribution of power measurements in order to fix the threshold for an appliance. It often happens that due to noise in the smart meters or devices, some measurements during short time intervals are either absent while the device is operating, or produce abnormal peaks during the OFF state. For this reason, to ensure a smoother behaviour, Kelly and Knottenbelt [32] set both a power threshold and a time threshold. The

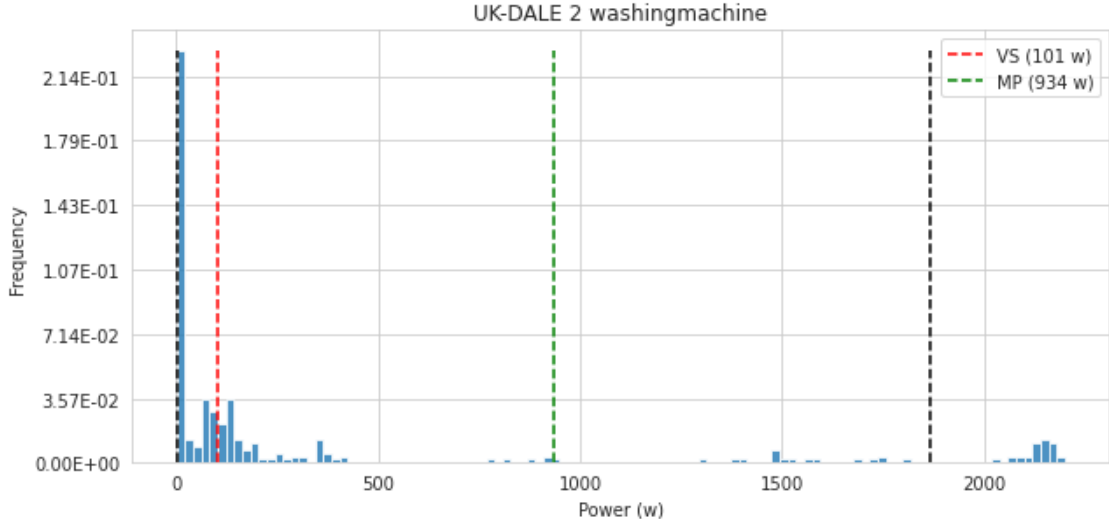


Figure 1: Distribution of a washing machine power load through all the monitoring time. The records pertain to house 2 of UK-DALE dataset. The graph was cropped vertically as 0 W consumption is more than 17% of the total number of records. Black dashed lines mark the centroids found by k -means clustering (1 watts and 1866 watts), while color dashed lines are the thresholds fixed by different methods.

power threshold could be fixed by MP or VS or fixed externally by hand as done in [32]. The time threshold $(\mu_0^{(\ell)}, \mu_1^{(\ell)})$ specifies the minimum length of time that device ℓ must be in a given state, e.g. if a sequence of power measurements are below $\lambda^{(\ell)}$ for a time $t < \mu_0^{(\ell)}$, then that sequence is considered to be in the previous state (ON in this binary case).

In [32], both power and time thresholds are chosen empirically, after analysing the appliance behaviour. Table 1 shows the values of the thresholds relevant to our work. The threshold λ is chosen usually at lower values, as the time threshold already filters noisy records. It would be desirable to turn this thresholding method into a fully automated data driven algorithm, in order to remove all subjective inputs.

Threshold	Dishwasher	Fridge	Washing machine
λ (W)	10	50	20
μ_0 (s)	30	1	3
μ_1 (s)	30	1	30

Table 1: Activation time (AT) threshold values used in this work, taken from [32].

Figure 2 compares the three thresholding methods. Each graph shows the three values of $\lambda^{(\ell)}$ for a given device, together with the result of applying each thresholding method to the same input series. Observe that the same power data gives rise to rather different series for the ON/OFF status depending on the choice of thresholding method. We thus see that there are multiple ways to define a classification problem given the input signal.

A comparison and a discussion of each thresholding method after training state-of-the-art NILM for regression and classification problems will be performed in Section 6.

4 Neural Networks

Almost all state of the art models propagate their inputs through one or more convolutional layers [33, 34]. This is done to ensure that the models are translation invariant. As NILM is related to time series, many studies also add recurrent layers (e.g. LSTM or GRU) to their networks [18, 21]. These layers tend to get very good results on sequence-related problems. In this work, we will try out two different models: one that relies purely on convolutions, and other that also applies recurrent layers after the convolutions.

It is important to stress that both of these neural networks can be applied to train a classification model to predict device status or a regression model to predict device power load, the only difference in their architecture lies in the last layer (see Figure 3b), where an additional softmax layer needs to be added for the classification problem.



Figure 2: Sample from the washing machine power load sequence, depicting how different thresholding methods classify each instance as ON or OFF.

4.1 Convolutional Network

Our first model relies solely on convolutional layers, inspired on the architecture from the work of Luca Massidda et al. [23]. The general scheme follows the classic approach to the semantic segmentation of images. See Figure 3a to better understand the following model explanation.

The CONV model receives as input a vector with size $L_{in} = 510$ which represents the household aggregated power over an $8\frac{1}{2}$ hour interval. The vector is propagated through an encoder, characterised by alternating convolution and pooling modules. Each encoder layer begins with a convolution of kernel size 3 and no padding, then applies batch normalization and ReLU activation, and ends with a max pooling of kernel size 2 and stride 2. Only the last layer omits the max pooling step. Encoder layers increase the space of the features of the signal at the cost of decreasing the temporal resolution.

After that, the *Temporal Pooling* module aggregates the features at different resolutions, which is reminiscent of inception networks [35]. Four different average poolings are applied, with kernel sizes 5, 10, 20 and 30; having the same stride as kernel size. Each of those layers then propagate their values through convolution layers of kernel size 1 and no padding, followed by a batch normalization and ReLU activation. All of their outputs are then concatenated.

Finally, the decoder module applies one convolution of kernel size 8 and stride 8, followed by batch normalization. It then bifurcates into two different outputs: the appliance status and the appliance power. Both outputs are computed by

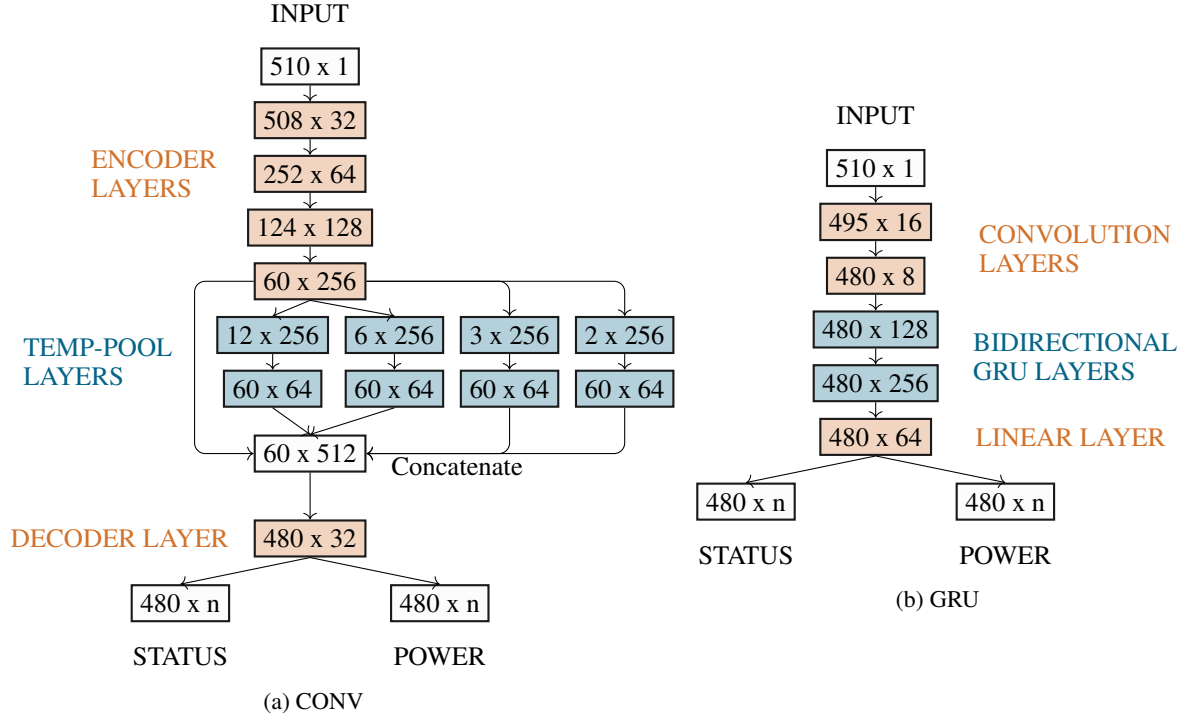


Figure 3: Architecture of each model. There are two possible outputs, the model trains differently depending of which output we chose.

propagating the network values through one last convolution layer of kernel size 1 and padding 1. In the case of status, we apply the softmax function. Both status and power load output vectors have the same sampling frequency as the input aggregate load, but have a shorter length $L_{out} = 480$ as explained in Section 5.

4.2 Bidirectional GRU Network

Some authors tend to connect convolutional and recurrent layers to extract temporal correlations out of the input sequence [24, 32]. This second model follows a prototypical GRU scheme, depicted in Figure 3b. The input and output layers are the same as in the previous model. For the processing units, the GRU model propagates the input vector through two convolutional layers with kernel size 20, padding 2 and stride 1, before applying the recurrent (bidirectional GRU) layers.

One can see that the model architecture is rather lightweight. However, GRU takes longer to train than CONV: adapting the GRU weights requires a lot of computation, compared to updating the weights of convolutional layers.

5 Methodology

5.1 Preprocessing

In order to make our results reproducible and easy to compare with other works, we restrict to the UK-DALE dataset [8], which is a standard benchmark for NILM.

Date of release	2014
Location	United Kingdom
Number of households	5
Meter units	Watts
Sampling frequency	6 seconds

Table 2: UK-DALE dataset features.

Building	1	2	3	4	5
Total time (days)	>365	235	39	206	137
Appliances	53	18	4	11	24

Table 3: UK-DALE dataset.

Only houses 1, 2 and 5 have been used for this work. Our target appliances which are found in the three buildings are: fridge, dishwasher and washing machine. This choice of houses and appliances is common in other works [23, 32, 36], as they seek to monitor appliances with distinguishable load absorption patterns and relevant contribution to the total power consumption.

Every power load series was downsampled from 6 seconds to 1 minute-frequency. After this downsampling, every input sequence comprises $8\frac{1}{2}$ hours of time, which amount to $L_{\text{in}} = 510$ records. Since the models use convolutions with no padding, the first and last records of each series are dropped in the output, thus leading to an output sequence having $L_{\text{out}} = 480$ records, i.e. 8 hours. We have divided the original time series into input sequences with an overlap of 30 records between consecutive input sequences, so that the output sequence are continuous in time and have no gaps. Aggregate power load is normalized, dividing the load by a reference power value of 2000 W for numerical stability. Each input series is further normalized by subtracting its mean. Thus, we can define the following input and output series for the regression problem

$$\text{Regression: } \quad \mathbf{x}_j = \frac{\mathbf{P}_j - \bar{P}_j}{2000}, \quad \mathbf{y}_j^{(\ell)} = \frac{\mathbf{P}_j^{(\ell)}}{2000}, \quad (5)$$

$$\text{where } \bar{P}_j = \frac{1}{L_{\text{in}}} \sum_{i=1}^{L_{\text{in}}} P_{j,i}.$$

To define the classification problem, the target $\mathbf{y}_j^{(\ell)}$ is the device status which is computed from $\mathbf{P}_j^{(\ell)}$ using the thresholding methods described in Section 3. More specifically, we have

$$\text{Classification: } \quad \mathbf{x}_j = \frac{\mathbf{P}_j - \bar{P}_j}{2000}, \quad \mathbf{y}_j^{(\ell)} = \mathbf{s}_j^{(\ell)}, \quad (6)$$

where $\mathbf{s}_j^{(\ell)}$ is a series of binary values defined by (2).

The training set for each problem is built by adding the first 80% sequences from each of the three buildings, which amounts to 1941 sequences (describing a total time of 687 days of measurements). The validation set is built by using the subsequent 10% records from house UK-DALE 1, for a total of 183 sequences (65 days), while the test set is composed of the last 10% sequences of the same building, having the same size as the validation set.

	Train	Validation	Test
Number of points (N)	1941	183	183
Total time (days)	687	65	65

Table 4: Training, validation and test sets. Each point is a pair $(\mathbf{x}_j, \mathbf{y}_j^{(\ell)})$ of time series, where \mathbf{x}_j has $L_{\text{in}} = 510$ records, and $\mathbf{y}_j^{(\ell)}$ has $L_{\text{out}} = 480$ records, both of them at 1 min. intervals.

In order to judge whether we are dealing with a balanced classification problem, it will be useful to report how often a given device has been ON during the training and test sets, depending on which thresholding method has been applied. The results can be seen in Table 5.

It is important to stress a number of things from the observation of this table. First, the fraction of ON states is clearly dependent on the thresholding method, as it was already clear from Figure 2. Next, dishwasher and washing machine are only sparsely activated, while the fridge is considered to be ON roughly half of the time. In these two cases we are dealing with an imbalanced class problem, which should be taken into account when defining and interpreting the appropriate metrics. Finally, in all cases but specially for the washing machine, the prevalence of the positive class differs greatly from the training to the test set. This of course could happen because these periods have been chosen consecutive in time (in accordance with other works). If the train-validation-test split was done randomly over the 2307 series records, we would observe a similar class distribution across sets. Splitting training and test sets for a time series in machine learning problems always involves a delicate choice: whether to split records randomly (which ensures homogeneous distribution) or chronologically (which is closer to the real operating conditions).

Threshold	Set	Dishwasher	Fridge	Washing Machine
MP	Train	0.77	42	0.97
	Test	0.62	46	1.70
VS	Train	0.83	44	1.80
	Test	0.67	47	2.50
AT	Train	2.30	42	4.60
	Test	2.40	45	7.30

Table 5: Fraction of activation time (in %) for each device over the train and test sets.

5.2 Training

Each of the models described in Section 4 was trained for 300 epochs. Training data was fed to the model in batches of 32 sequences, shuffled randomly.

The loss function for the regression problem is the mean square error or L2 metric, given by

$$\mathcal{L}_{\text{reg}}^{(\ell)} = \frac{1}{N_{\text{train}}} \sum_{j=1}^{N_{\text{train}}} \frac{1}{L_{\text{out}}} \sum_{i=1}^{L_{\text{out}}} \left(y_{j,i}^{(\ell)} - \hat{y}_{j,i}^{(\ell)} \right)^2. \quad (7)$$

The standard choice of loss function for the classification problem is binary cross entropy:

$$\mathcal{L}_{\text{class}}^{(\ell)} = \frac{1}{N_{\text{train}}} \sum_{j=1}^{N_{\text{train}}} \frac{1}{L_{\text{out}}} \sum_{i=1}^{L_{\text{out}}} \left(y_{j,i}^{(\ell)} \cdot \log \hat{y}_{j,i}^{(\ell)} + (1 - y_{j,i}^{(\ell)}) \cdot \log(1 - \hat{y}_{j,i}^{(\ell)}) \right), \quad (8)$$

where $\hat{y}_j^{(\ell)}$ is the probability that device ℓ is ON at each time step.

During the 300 training epochs, we keep the model that achieves the minimum loss over the validation set, using an Adam optimizer for weights update, with a starting learning rate of $1E - 4$.

Both data preprocessing and neural network training were performed on Python. Specifically, the models were written on Pytorch and trained in a GPU NVidia GeForce GTX 1080 with 8 GB of VRAM, NVIDIA-SMI 440.95.01 and CUDA v10.2. The code for this paper is available online⁴ and the data comes from a public dataset, so all results reported in this paper are reproducible. Using the configuration stated in this section, CONV models took from 7 to 8 minutes to train 300 epochs, while GRU architectures took 16 minutes.

5.3 Metrics

Although metrics are clearly related to loss functions used for model training, the main difference is that the reported metrics are not required to be differentiable. When the output is a continuous variable (power load in our case), we use as the relevant metric the L1 error or MAE rather than RMSE, since the latter tends to give too much importance to large deviations.

$$\text{MAE}^{(\ell)} = \frac{1}{N_{\text{train}}} \sum_{j=1}^{N_{\text{train}}} \frac{1}{L_{\text{out}}} \sum_{i=1}^{L_{\text{out}}} \left| y_{j,i}^{(\ell)} - \hat{y}_{j,i}^{(\ell)} \right|, \quad (9)$$

When the output variable is categorical, we can use the F_1 -score to balance precision and recall in balanced problems where there is no preference to achieve a better classification of the ON or OFF classes. The F_1 -score is the harmonic mean of precision and recall, or directly

$$F_1^{(\ell)} = \frac{1}{N_{\text{test}}} \sum_{j=1}^{N_{\text{test}}} \frac{TP_j^{(\ell)}}{TP_j^{(\ell)} + \frac{1}{2}(FP_j^{(\ell)} + FN_j^{(\ell)})} \quad (10)$$

⁴Open-source repository: https://github.com/UCA-Datalab/better_nilms

where the true positives (TP), false positives (FP), true negatives (TN) and false negatives (FN) in each series are given by

$$\begin{aligned} TP_j^{(\ell)} &= \sum_{i=1}^{L_{\text{out}}} \hat{s}_{j,i}^{(\ell)} \cdot y_{j,i}^{(\ell)}, & FP_j^{(\ell)} &= \sum_{i=1}^{L_{\text{out}}} \hat{s}_{j,i}^{(\ell)} \cdot (1 - y_{j,i}^{(\ell)}), \\ FN_j^{(\ell)} &= \sum_{i=1}^{L_{\text{out}}} (1 - \hat{s}_{j,i}^{(\ell)}) \cdot y_{j,i}^{(\ell)}, & TN_j^{(\ell)} &= \sum_{i=1}^{L_{\text{out}}} (1 - \hat{s}_{j,i}^{(\ell)}) \cdot (1 - y_{j,i}^{(\ell)}). \end{aligned}$$

where in this case $y_{j,i}^{(\ell)}$ is the state of device ℓ at instant i , and $\hat{s}_{j,i}^{(\ell)}$ is the predicted state as defined by

$$\hat{s}_{j,i}^{(\ell)} = I \left(\hat{y}_{j,i}^{(\ell)} - 0.5 \right). \quad (11)$$

For imbalanced problems, such as NILM for the dishwasher and washing machine (see Table 5), the F_1 -score might not be the best metric to report. Rather, since those devices are ON roughly 1% of the time, it is better to consider a suitable metric for imbalanced classification problems, like the area under the ROC curve. [37].

6 Results

6.1 Regression problem

We begin our discussion of results by reporting the metrics obtained over the test set by the two models (CONV and GRU) in the regression problem for each of the three appliances $\ell = \{\text{dishwasher, fridge, washing machine}\}$.

Model	Dishwasher	Fridge	Washing Machine
CONV	11.59	26.95	18.25
GRU	8.07	28.68	15.00

Table 6: MAE scores (in watts) for regression models on each appliance

The analysis of these metrics needs a word of caution: it is natural to expect that if a device has been sparsely activated during the test set, the predicted load will give an overall lower MAE than a similar device that has been used more often (see Table 5). For this reason, some authors have suggested other metrics such as the energy error [38, 39]. For a recent review of all metrics that have been used in NILM, see [27].

To understand the complexity of disaggregating the power signal in NILM, we have plotted a time series from the test set in Figure 4. In the plots we show the input signal \mathbf{P}_j (aggregated power load), together with the real power of each device $\mathbf{P}_j^{(\ell)}$ and the predicted power obtained from the CONV network $\hat{\mathbf{P}}_j^{(\ell)}$.

In the first graph of Figure 4 we see that the model has identified correctly the two main power peaks of 2200 W corresponding to the dish washer, but has properly ignored other similar large peaks occurring earlier in the series. In the second graph, we observe that the fridge power prediction is often masked by the presence of other devices, having a mean value of just 100 W but a very periodic activation pattern. When the aggregate power load is small, the model is able to better resolve the signal coming from the fridge. The washing machine has a more complex consumption pattern during its activation period, but the model has also been able to identify correctly the activation peaks while ignoring other similar peaks of the same magnitude occurring earlier in the series that do not correspond to washing machine operation.

6.2 Classification problem

As we have mentioned above, the classification problem is not uniquely defined since the raw data do not include the real intervals where each device was ON/OFF, but only its consumption. Thus, we have three different classification problems depending on the choice of thresholding methods described in Section 3. For each possible value of (model, thresholding, device) we report the F_1 -score (10) over the test set in Table 7.

The next to last line shows that our results are in good agreement with those reported by the authors of [23]. Also, we can observe that CONV has a slightly better F_1 -score than GRU for the classification problems in all three devices and thresholding methods, although both of them show a very good performance (see Figure 5). In general, the classification

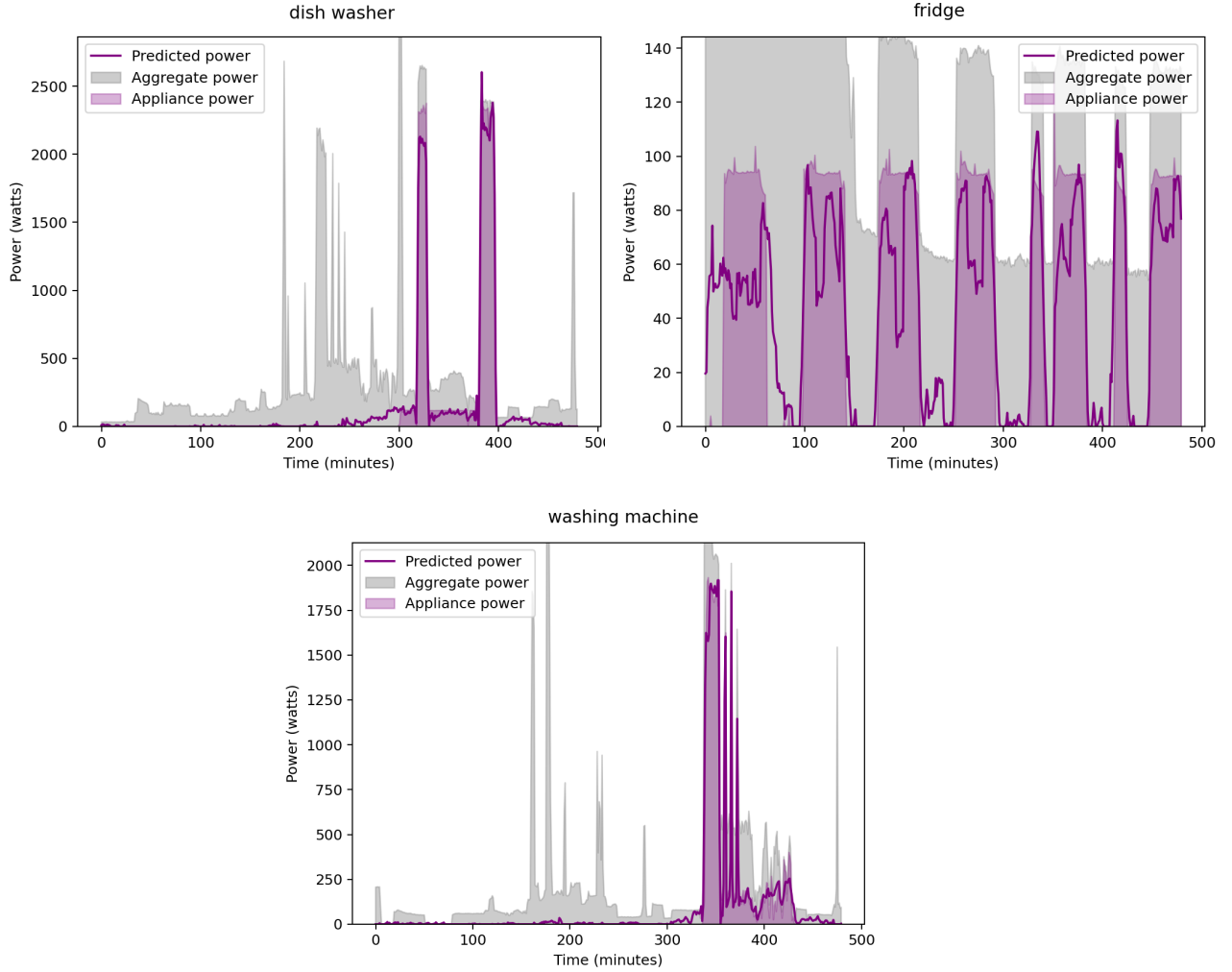


Figure 4: CONV regression: aggregated power load (input signal) and real and predicted loads for each device.

Threshold	Model	Dishwasher	Fridge	Washing Machine
MP	CONV	0.93	0.87	0.93
	GRU	0.84	0.87	0.87
VS	CONV	0.93	0.87	0.88
	GRU	0.84	0.87	0.82
AT	CONV	0.91	0.86	0.97
	GRU	0.90	0.86	0.96

 Table 7: F_1 -scores for classification models on each appliance and threshold

problem for the fridge is harder, for reasons that have been already mentioned above. We raised the idea of using AUC over F_1 -score in Section 5.3. We computed AUC and realized it was almost identical to F_1 -score, so we will keep using the latter as it is more common in the literature.

It is also instructive to represent the input signal \mathbf{P}_j , together with the real output signal $\mathbf{P}_j^{(\ell)}$ describing the status of device ℓ and the predicted status $\hat{s}_j^{(\ell)}$, to grasp the nature of NILM problem for classification. We have plotted in Figure 5 the output of CONV on a given series of records from the test set where the three devices have been activated (sometimes simultaneously). Observe that the model is able to discriminate, with a very good precision, the periods in which each of the devices are activated, just from the observation of the aggregated power signal.

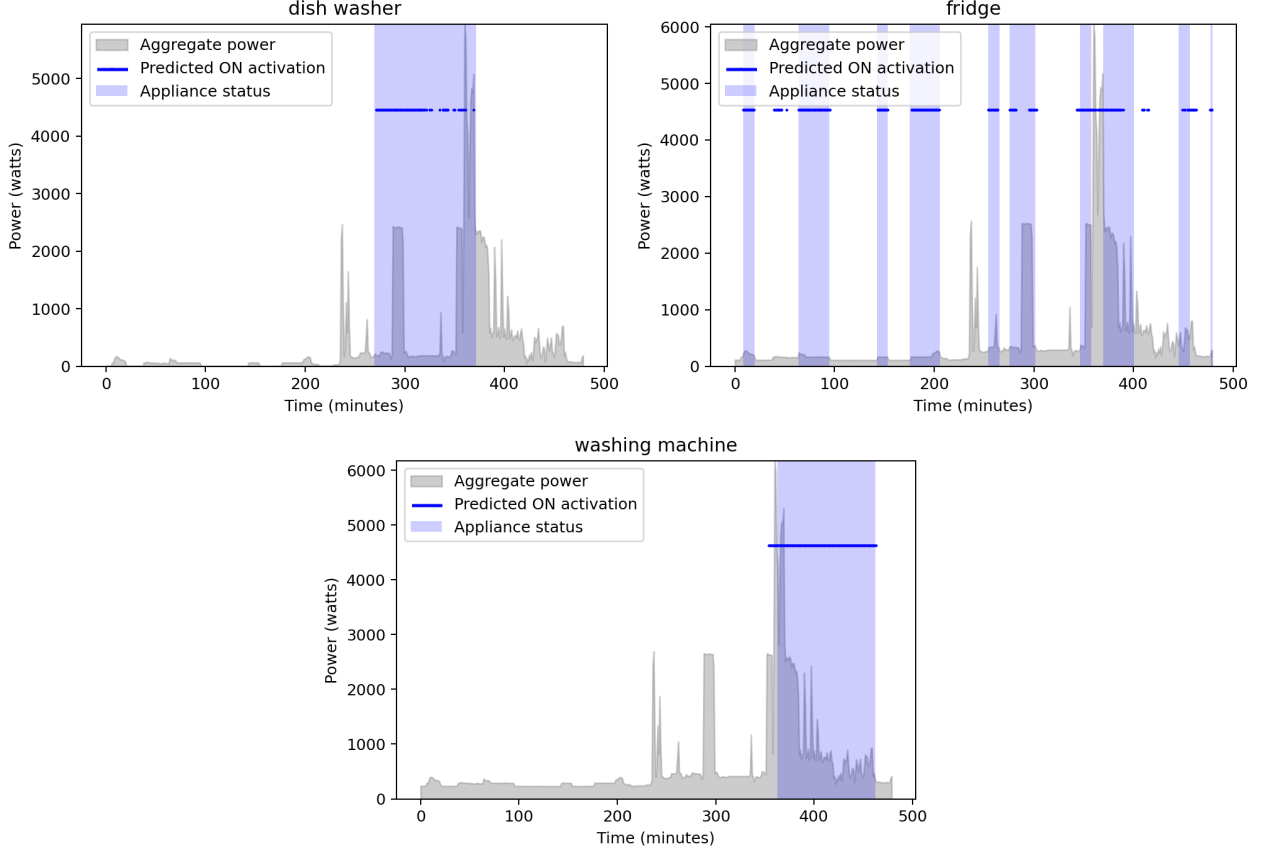


Figure 5: CONV model applying AT threshold: aggregated power load (input signal), real device status (output signal) and predicted status.

6.3 Reconstructing the power signal

A very natural question to address is which of the three proposed thresholding methods should be preferred. One would naively think that the one leading to a better F_1 -score would be the best choice, if this was only based on prediction performance. However, placing a trivial threshold of zero would yield state ON for all time intervals at the training and test sets, and any decent ML method would immediately learn this, thus reaching a perfect F_1 -score but having no useful interpretation at all. Thus, we need to balance predictive performance with a way of judging which method is more meaningful. In the absence of any other external information on when each device can be considered to be ON or OFF, we need to find an objective quantitative argument to tackle this question.

For this purpose, we propose to reconstruct the power signal from each device and compare the reconstructed signal with the original power load of the device. We compute the average power $\bar{P}_{ON}^{(\ell)}$, (resp. $\bar{P}_{OFF}^{(\ell)}$) for device ℓ during the periods that are considered to be ON, (resp. OFF) after applying the thresholding method, and reconstruct the power series with these binary values.

More specifically, we have

$$\bar{P}_{ON}^{(\ell)} = \frac{1}{N_{\text{train}}} \sum_{j=1}^{N_{\text{train}}} \frac{1}{L_{\text{out}}} \sum_{i=1}^{L_{\text{out}}} s_{j,i}^{(\ell)} P_{j,i}, \quad (12)$$

$$\bar{P}_{OFF}^{(\ell)} = \frac{1}{N_{\text{train}}} \sum_{j=1}^{N_{\text{train}}} \frac{1}{L_{\text{out}}} \sum_{i=1}^{L_{\text{out}}} (1 - s_{j,i}^{(\ell)}) P_{j,i}, \quad (13)$$

and reconstruct a binary power load for device ℓ as

$$\mathbf{BP}_j^{(\ell)} = \bar{P}_{ON}^{(\ell)} \mathbf{s}_j^{(\ell)} + \bar{P}_{OFF}^{(\ell)} (1 - \mathbf{s}_j^{(\ell)}) \quad (14)$$

The reconstructed power series can be seen, together with the original series in Figure 6 for two of the thresholding methods, corresponding to the same data as Figure 2.

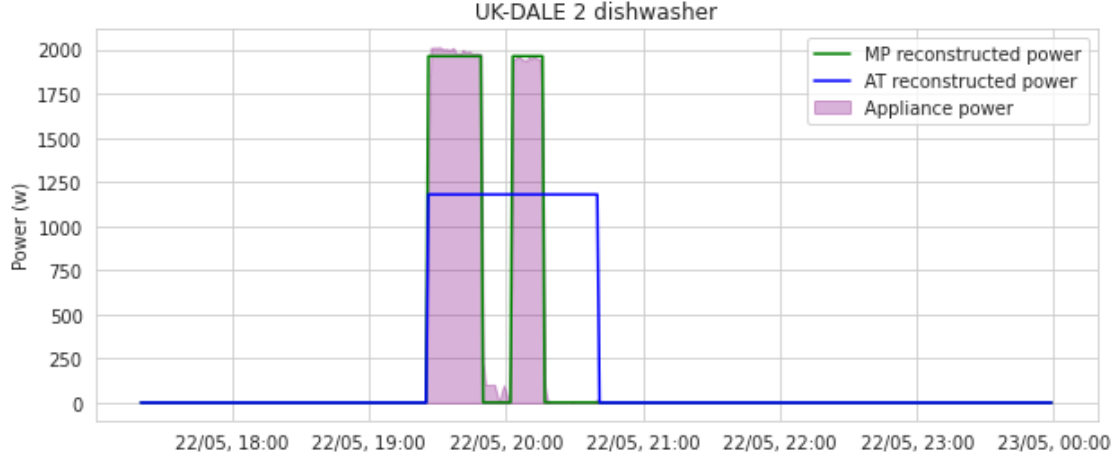


Figure 6: Device power load reconstruction from two different thresholding methods.

We can compute the MAE between the original $P^{(\ell)}$ and reconstructed series $\mathbf{BP}^{(\ell)}$ averages over the training set, which we call the *intrinsic error*, since it is prior to any prediction method. The results for the three devices and thresholding methods are shown in Table 8.

Threshold	Dishwasher	Fridge	Washing machine
MP	3.48	4.67	3.96
VS	4.39	4.71	6.60
AT	26.37	4.66	7.42

Table 8: Intrinsic error: MAE between the original and reconstructed power series.

From this comparison, we see that the Activation Time (AT) thresholding is the one having the largest intrinsic error, while Middle Point (MP) thresholding offers the closest reconstructed power series. The fridge has similar intrinsic error for all three methods since the original series is very regular, being almost a binary series itself (see Figure 4).

As we mentioned above, it is not enough to look only at the classification metrics in Table 7 to judge which is the best thresholding method for a NILM problem. For this reason, given the prediction output of the classification problem, we compute the reconstructed binary series and compare it with the original power series. MAE averaged over the test set are reported in Table 9 for the two models (GRU and CONV).

Threshold	Model	Dishwasher	Fridge	Washing Machine
MP	CONV	9.09	21.45	39.45
	GRU	11.25	21.80	41.66
VS	CONV	9.25	21.01	40.74
	GRU	11.59	22.19	41.85
AT	CONV	19.75	21.26	57.23
	GRU	21.07	22.45	56.35

Table 9: MAE scores (in watts) for classification models after reconstructing the power load, on each appliance and threshold.

The first thing to note is that naturally the MAE errors are larger than the intrinsic errors, as they incorporate the errors in the classification. However, it is worth noting that for the dishwasher in AT thresholding this error is actually smaller than the intrinsic one. We find the explanation for that phenomenon in Figure 6: current AT parameters contain a large time threshold for the dishwasher (see Table 1), which might lead to incorrect thresholding and large deviations in the reconstructed series. This suggests that the free parameters in AT thresholding should be optimized by minimizing

the intrinsic error for each device over the training set. As shown in previous tables, CONV has a slightly better performance than GRU. It is also worth noting that the MAE for the washing machine has increased by a factor of 10 with respect to the intrinsic error, while in the other two devices, the factor is close to 4. The most likely explanation for this deviation is due to the train-test splitting: most of the error comes from activation periods, and these occur twice more often in the test than in the training set for the washing machine (see Table 5) while there is hardly no variation in the other two devices. This brings back the already mentioned remark on the importance of having a train-test split that preserves the distribution of classes.

Finally, these MAE values should be compared with the ones obtained by training our models for a pure regression problem (see Table 6). We observe that the results are comparable, and for the fridge they are even better in the reconstructed case. The explanation comes from the fact that the raw power signal for the fridge is almost binary, so the reconstructed signal matches this behaviour properly and the ON/OFF values \bar{P}_{ON} and \bar{P}_{OFF} calculated over the training set are very close to the real values. Thus, in this case good metrics for the classification problem immediately translate into good MAE for the reconstructed series. By contrast, addressing the regression problem is harder for the fridge, where the regression curve often fails to reconstruct this signal, specially when it is masked by larger signals coming from other devices (see Figure 4b).

6.4 Classification metrics on the regression problem

In the last section we trained the model for classification but evaluated the MAE for the reconstructed power signal and compared it with the MAE obtained by directly training the model for regression. Now we do the opposite: we apply the thresholding methods on the real and predicted power signal to obtain the real and predicted status at each time interval, and then we calculate the F_1 metric over these values. The results can be seen in Table 10.

Threshold	Model	Dishwasher	Fridge	Washing Machine
MP	CONV	0.89	0.77	0.93
	GRU	0.90	0.74	0.91
VS	CONV	0.77	0.78	0.81
	GRU	0.81	0.75	0.83
AT	CONV	0.09	0.76	0.46
	GRU	0.27	0.72	0.65

Table 10: F_1 -scores for regression models after thresholding, on each appliance and threshold

These scores are on average worse than the ones from the original classification approach (Table 7). In particular, F_1 -scores of AT for dishwasher and washing machine are extremely low, which is caused by the small power threshold set by the thresholding formulation (see Table 1). During periods of inactivity, regression models output values that, although being relatively small compared to the power peaks of dishwasher and washing machine, are high enough to surpass the AT power threshold, thus triggering the ON state and causing many FPs.

7 Balancing classification and regression

So far we have trained our models to solve a pure classification or regression problem. However, as we explained in Section 4, our network architectures contain two different output layers, one for regression and the other for classification. This means that we can also train the model to solve both problems simultaneously, with a weighted combined loss function. The total loss of the model would then be:

$$\mathcal{L}_{\text{tot}}^{(\ell)} = w \cdot \mathcal{L}_{\text{class}}^{(\ell)} + (1 - w) \cdot \mathcal{L}_{\text{reg}}^{(\ell)}/k, \quad (15)$$

where $\mathcal{L}_{\text{class}}^{(\ell)}$ is the binary cross entropy (8), $\mathcal{L}_{\text{reg}}^{(\ell)}$ is the MSE (7), and k is a constant to normalize both losses so that they have comparable magnitude, estimated to be $k = 0.0066$. The constant $w \in [0, 1]$ allows to shift between pure classification and regression.

We train both models using different values of the weight w with MP thresholding. Other thresholding methods showed a similar behaviour. For each value of w , the model is trained five times with random weight initializations, as explained in Section 5. We show the output metrics MAE and F_1 -score for varying w in the figures below.

Note that when $w = 0$ the model does not train for classification. For this reason, we include for $w = 0$ a single point for the F_1 curve, corresponding to applying the thresholding method on the regression output, as we did in Section 6.4.

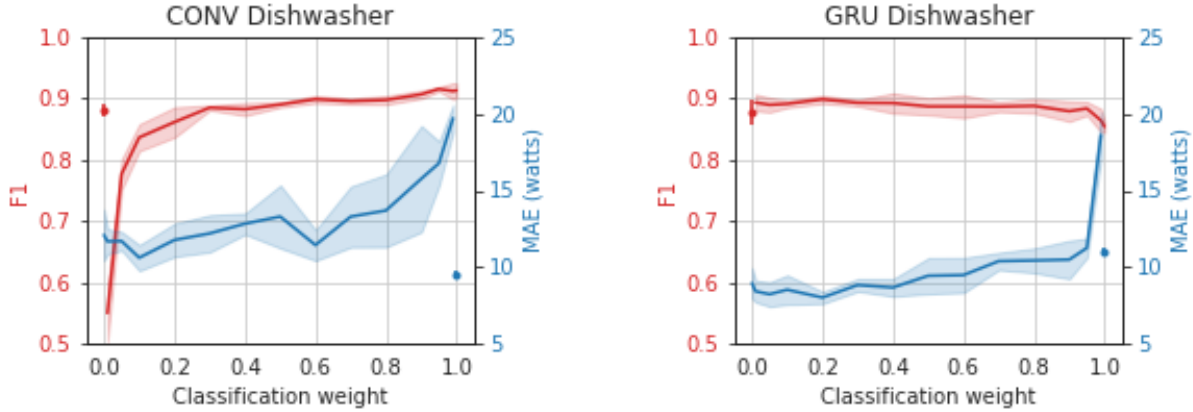


Figure 7: Model scores for dishwasher depending on classification weight

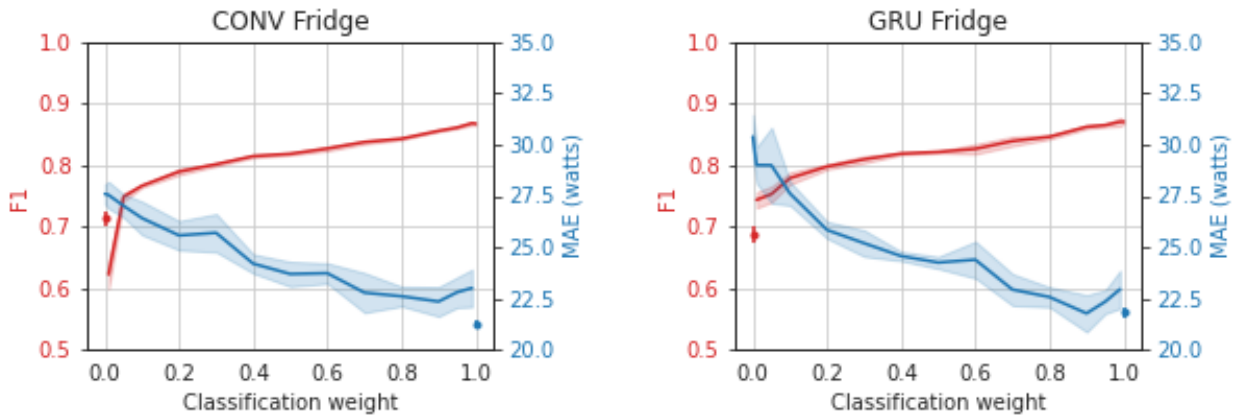


Figure 8: Model scores for fridge depending on classification weight

Likewise, for $w = 1$ the model does not train for regression. For this reason, we include for $w = 1$ the MAE obtained by reconstructing the power signal from the classification output, as explained in Section 6.3.

Looking at the results in Figures 7–9 we observe a very different behaviour for the fridge than for the other two devices, due to their different characteristics already mentioned. In the dishwasher and washing machine, the F_1 -score grows monotonically with w for CONV as one would expect, but is almost constant for GRU, with a small drop for values of w close to 1 which are hard to explain. Likewise, the MAE in both models and devices tends to grow for larger w , which is natural since the model has a smaller weight for the regression problem. As for the extra points in the graphs, for the dishwasher we see that the F_1 -score obtained by thresholding a pure regression output (red dot) is comparable to the best score obtained by larger weights in classification. Rather surprisingly, the reconstructed power signal from pure classification output (blue dot) has a lower MAE than the best regression weight for CONV and still a comparable value in GRU. This discussion also holds for the washing machine, except the reconstructed series behaves poorly in this case, as we have already discussed by the activation pattern of the signal (see Table 9 and the ensuing remarks). For the fridge, the behaviour is consistent for both models, but different from the other two devices. While the F_1 -score behaves similarly, the MAE for regression decreases with w , which is clearly counter-intuitive: the model prioritizes classification loss, and in doing so it performs better in the regression problem as well. Also, the purely reconstructed signal for $w = 1$ (blue dot) has a better MAE than any of the models trained for regression. This fact can again be explained by the second graph in Figure 4: the regular (almost binary) activation pattern of the fridge is much better captured by a classification model with the right threshold than by a regression model, since the weak signal of the fridge is often masked by that of other devices.

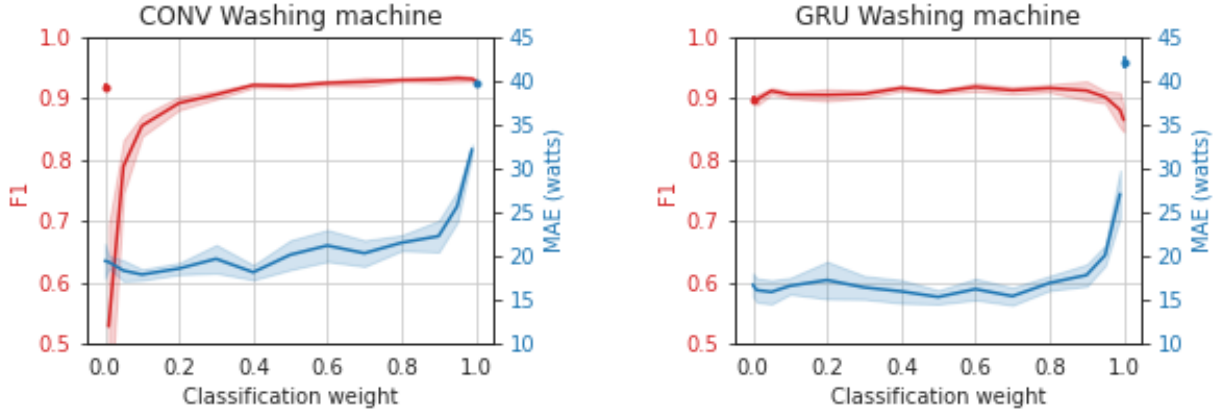


Figure 9: Model scores for washing machine depending on classification weight

8 Summary and conclusions

Non Intrusive Load Monitoring is typically framed as a classification problem, where the input data is the aggregated power load of the household and the output data is the sequence of ON/OFF states of a given monitored device. It is important to stress that this problem is derived, as the raw data do not contain the variable that needs to be predicted but only the power consumption. Creating a classification problem from the raw power signal data requires an external determination of the status by some thresholding method. We have discussed three possible methods in Section 3 and how they lead to classification problems with different results.

A discussion of what is the most appropriate method should not be based on the performance achieved by prediction models alone, but include also some objective way to judge the interpretability of the results. We suggest as an objective criterion to use the intrinsic error, i.e. MAE between the original power series and reconstructed binary series.

We show that deep learning models can be trained to minimize the regression loss (7) or the classification loss (8), but it is also possible to combine both into a weighted loss introducing an extra hyperparameter. This parameter balances the weight given to both problems, that are effectively solved both at a time. The optimal choice of this parameter depends strongly on the characteristics of the device.

To conclude we would like to mention possible improvements and future extensions of this work.

First, two of the thresholding methods (MP and VS) are entirely algorithmic, but AT needs some external parameters to be fixed. We suggest that these free parameters, the time thresholds $(\mu_0^{(\ell)}, \mu_1^{(\ell)})$ for each device, should be fine tuned to minimize the intrinsic error defined in Section 6.3.

Second, some of the results highlight the importance of discussing chronological vs. random splitting of records to form the training, validation and test sets. This choice will become less significant in the large data size limit, but for moderate sizes they can still lead to different results. Similar issues are key in discussing fraud detection methods, where fraud techniques evolve in time and differ chronologically throughout the time span of the dataset.

Finally, we have chosen to address the simpler NILM problem of recognising the same devices seen in the training and test sets. Training models on certain households and generalizing to unseen devices in different households is a harder problem that lies at the root of industrial large scale applications of NILM.

Our purpose for this paper was to highlight an important factor at the foundations of NILM as a supervised learning problem, so we focused on a simple, well known benchmark dataset. We envisage to extend our study to larger, more recent datasets like Pecan Street [40] or ECO [41], addressing also the generalization capacity of deep learning models to cope with unseen devices in households not present in the training set.

9 Acknowledgements

This research has been financed in part by the Spanish MICINN under grants PGC2018-096504-B-C33 and RTI2018-100754-B-I00 and the European Union under the 2014-2020 ERDF Operational Programme and by the Department of

Economy, Knowledge, Business and University of the Regional Government of Andalusia (project FEDER-UCA18-108393). DP gratefully acknowledges an Industrial PhD grant from Universidad de Cádiz.

References

- [1] George William Hart. Nonintrusive appliance load monitoring. *Proceedings of the IEEE*, 80(12):1870–1891, 1992.
- [2] Christoforos Nalmpantis and Dimitris Vrakas. Machine learning approaches for non-intrusive load monitoring: from qualitative to quantitative comparison. *Artificial Intelligence Review*, 52, 01 2018.
- [3] Pedro Paulo Marques do Nascimento. Applications of deep learning techniques on nilm. *Diss. Universidade Federal do Rio de Janeiro*, 2016.
- [4] Christoph Klemenjak and Peter Goldsborough. Non-intrusive load monitoring: A review and outlook, 2016.
- [5] Federal energy regulatory commission assessment of demand response and advanced metering, 2018.
- [6] Zico Kolter and Matthew Johnson. Redd: A public data set for energy disaggregation research. *Artif. Intell.*, 25, 2011.
- [7] Kyle Anderson, Adrian Ocneanu, Diego Benitez, Derrick Carlson, Anthony Rowe, and Mario Bergés. Blued: A fully labeled public dataset for event-based non-intrusive load monitoring research. *Proceedings of the 2nd KDD Workshop on Data Mining Applications in Sustainability (SustKDD)*, pages 1–5, 2012.
- [8] Jack Kelly and William Knottenbelt. The UK-DALE dataset, domestic appliance-level electricity demand and whole-house demand from five UK homes. 2(150007), 2015.
- [9] Christoph Klemenjak, Andreas Reinhardt, Lucas Pereira, Stephen Makonin, Mario Bergés, and Wilfried Elmenreich. Electricity consumption data sets: Pitfalls and opportunities. pages 159–162, 11 2019.
- [10] Christoph Klemenjak, Stephen Makonin, and Wilfried Elmenreich. Towards comparability in non-intrusive load monitoring: On data and performance evaluation, 2020.
- [11] Jorge Revuelta Herrero, Álvaro Lozano Murciego, Alberto Barriuso, Daniel Hernández de la Iglesia, G. Villarrubia, Juan Corchado Rodríguez, and Rita Carreira. Non intrusive load monitoring (nilm): A state of the art. pages 125–138, 06 2018.
- [12] Anthony Faustine, Nerey Henry Mvungi, Shubi Kaijage, and Kisangiri Michael. A survey on non-intrusive load monitoring methodologies and techniques for energy disaggregation problem, 2017.
- [13] Hyungsul Kim, Manish Marwah, Martin Arlitt, Geoff Lyon, and Jiawei Han. Unsupervised disaggregation of low frequency power measurements. *Proc. SIAM Conf. Data Mining*, 11:747–758, 2011.
- [14] J Zico Kolter and Tommi Jaakkola. Approximate inference in additive factorial hmms with application to energy disaggregation. In *Artificial intelligence and statistics*, pages 1472–1482, 2012.
- [15] Ruoxi Jia, Yang Gao, and Costas J Spanos. A fully unsupervised non-intrusive load monitoring framework. In *2015 IEEE International Conference on Smart Grid Communications (SmartGridComm)*, pages 872–878. IEEE, 2015.
- [16] M. A. Mengistu, A. A. Girmay, C. Camarda, A. Acquaviva, and E. Patti. A cloud-based on-line disaggregation algorithm for home appliance loads. *IEEE Transactions on Smart Grid*, 10(3):3430–3439, 2019.
- [17] Daniel Kelly. Disaggregation of domestic smart meter energy data. 2016.
- [18] Jihyun Kim, Thi-Thu-Huong Le, and Howon Kim. Nonintrusive load monitoring based on advanced deep learning and novel signature. In *Comp. Int. and Neurosc.*, 2017.
- [19] Odysseas Krystalakos, Christoforos Nalmpantis, and Dimitris Vrakas. Sliding window approach for online energy disaggregation using artificial neural networks. pages 1–6, 07 2018.
- [20] Alon Harell, Stephen Makonin, and Ivan V. Bajić. Wavenilm: A causal neural network for power disaggregation from the complex power signal, 2019.
- [21] M. Kaselimi, N. Doulamis, A. Doulamis, A. Voulodimos, and E. Protopapadakis. Bayesian-optimized bidirectional lstm regression model for non-intrusive load monitoring. In *ICASSP 2019 - 2019 IEEE International Conference on Acoustics, Speech and Signal Processing (ICASSP)*, pages 2747–2751, 2019.
- [22] Lamprini Kyrkou, Christoforos Nalmpantis, and Dimitris Vrakas. *Imaging Time-Series for NILM*, pages 188–196. 05 2019.

- [23] Luca Massidda, Marino Marrocu, and Simone Manca. Non-intrusive load disaggregation by convolutional neural network and multilabel classification. *Applied Sciences*, 10:1454, 02 2020.
- [24] Odysseas Krystalakos, Christoforos Nalmpantis, and Dimitris Vrakas. Sliding window approach for online energy disaggregation using artificial neural networks. pages 1–6, 07 2018.
- [25] P. Ducange, F. Marcelloni, and M. Antonelli. A novel approach based on finite-state machines with fuzzy transitions for nonintrusive home appliance monitoring. *IEEE Transactions on Industrial Informatics*, 10(2):1185–1197, 2014.
- [26] W. Kong, Z. Y. Dong, D. J. Hill, F. Luo, and Y. Xu. Improving nonintrusive load monitoring efficiency via a hybrid programing method. *IEEE Transactions on Industrial Informatics*, 12(6):2148–2157, 2016.
- [27] Lucas Pereira and Nuno Nunes. Performance evaluation in non-intrusive load monitoring: Datasets, metrics, and tools-a review. *Wiley Interdisciplinary Reviews: Data Mining and Knowledge Discovery*, page e1265, 05 2018.
- [28] Stephen Makonin and Fred Popowich. Nonintrusive load monitoring (nilm) performance evaluation. *Energy Efficiency*, 8(4):809–814, 2015.
- [29] Antonio Ruano, Alvaro Hernandez, Jesús Ureña, Maria Ruano, and Juan García. Nilm techniques for intelligent home energy management and ambient assisted living: A review. *Energies*, 12:2203, 06 2019.
- [30] Sanket Desai, Rabei Alhadad, Abdun Mahmood, Naveen Chilamkurti, and Seungmin Rho. Multi-state energy classifier to evaluate the performance of the nilm algorithm. *Sensors*, 19:5236, 11 2019.
- [31] James MacQueen et al. Some methods for classification and analysis of multivariate observations. In *Proceedings of the fifth Berkeley symposium on mathematical statistics and probability*, volume 1, pages 281–297. Oakland, CA, USA, 1967.
- [32] Jack Kelly and William Knottenbelt. Neural nilm: Deep neural networks applied to energy disaggregation. 11 2015.
- [33] Deyvison de Paiva Penha and Adriana Rosa Garcez Castro. Convolutional neural network applied to the identification of residential equipment in non-intrusive load monitoring systems. In *3rd International Conference on Artificial Intelligence and Applications*, pages 11–21, 2017.
- [34] Y. Yang, J. Zhong, W. Li, T. Aaron Gulliver, and S. Li. Semisupervised multilabel deep learning based nonintrusive load monitoring in smart grids. *IEEE Transactions on Industrial Informatics*, 16(11):6892–6902, 2020.
- [35] Christian Szegedy, Wei Liu, Yangqing Jia, Pierre Sermanet, Scott Reed, Dragomir Anguelov, Dumitru Erhan, Vincent Vanhoucke, and Andrew Rabinovich. Going deeper with convolutions, 2014.
- [36] Changho Shin, Sunghwan Joo, Jaeryun Yim, Hyoseop Lee, Taesup Moon, and Wonjong Rhee. Subtask gated networks for non-intrusive load monitoring. In *Proceedings of the AAAI Conference on Artificial Intelligence*, volume 33, pages 1150–1157, 2019.
- [37] Tom Fawcett. An introduction to roc analysis. *Pattern recognition letters*, 27(8):861–874, 2006.
- [38] Ebony T Mayhorn, Gregory P Sullivan, Joseph M Petersen, Ryan S Butner, and Erica M Johnson. Load disaggregation technologies: real world and laboratory performance. *Pacific Northwest National Laboratory (PNNL), Richland, WA (US), Tech. Rep. PNNL-SA-116560*, 2016.
- [39] Nipun Batra, Jack Kelly, Oliver Parson, Haimonti Dutta, William Knottenbelt, Alex Rogers, Amarjeet Singh, and Mani Srivastava. Nilmtk: an open source toolkit for non-intrusive load monitoring. In *Proceedings of the 5th international conference on Future energy systems*, pages 265–276, 2014.
- [40] Oliver Parson, Grant Fisher, April Hersey, Nipun Batra, Jack Kelly, Amarjeet Singh, William Knottenbelt, and Alex Rogers. Dataport and nilmtk: A building data set designed for non-intrusive load monitoring. 12 2015.
- [41] Wilhelm Kleiminger, Christian Beckel, and Silvia Santini. Household occupancy monitoring using electricity meters. In *Proceedings of the 2015 ACM International Joint Conference on Pervasive and Ubiquitous Computing (UbiComp 2015)*, Osaka, Japan, September 2015.